

Accepted Manuscript

Microstructure evolution of a Zn-Al coating co-deposited on low-carbon steel by pack cementation

Qi Xue, Cai yuan Sun, Jia Yan Yu, Ling Huang, Jun Wei, Jin Zhang



PII: S0925-8388(16)34220-7

DOI: [10.1016/j.jallcom.2016.12.291](https://doi.org/10.1016/j.jallcom.2016.12.291)

Reference: JALCOM 40213

To appear in: *Journal of Alloys and Compounds*

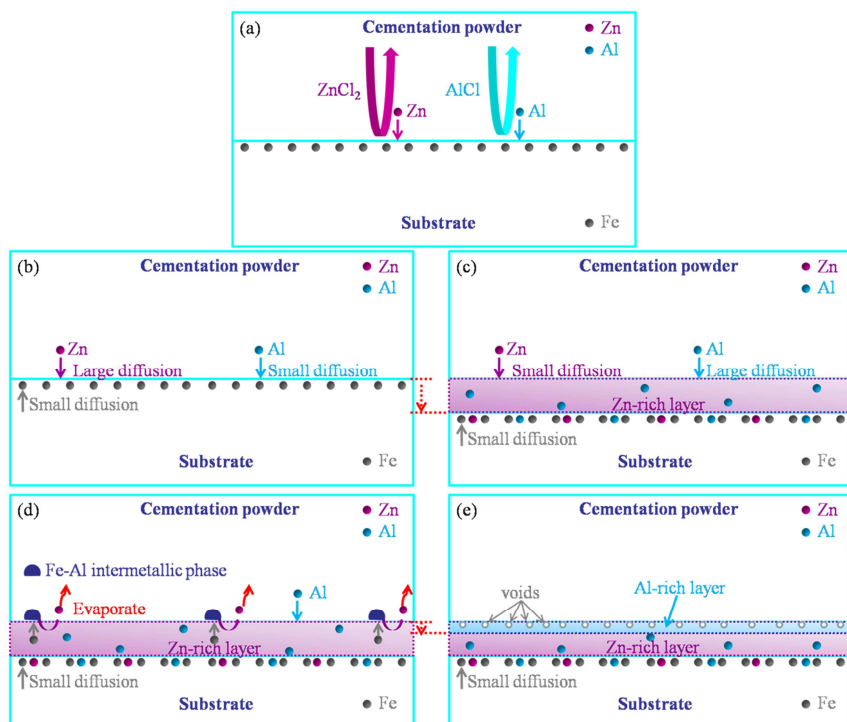
Received Date: 9 May 2016

Revised Date: 17 December 2016

Accepted Date: 22 December 2016

Please cite this article as: Q. Xue, C.y. Sun, J.Y. Yu, L. Huang, J. Wei, J. Zhang, Microstructure evolution of a Zn-Al coating co-deposited on low-carbon steel by pack cementation, *Journal of Alloys and Compounds* (2017), doi: 10.1016/j.jallcom.2016.12.291.

This is a PDF file of an unedited manuscript that has been accepted for publication. As a service to our customers we are providing this early version of the manuscript. The manuscript will undergo copyediting, typesetting, and review of the resulting proof before it is published in its final form. Please note that during the production process errors may be discovered which could affect the content, and all legal disclaimers that apply to the journal pertain.



Prime novelty statement

The effect of Al concentration on the morphologies of Zn-Al co-deposited coatings prepared on low carbon steel by pack cementation was investigated, which, hopefully, is to provide guidance to have a better understanding of the features about such a coating and optimise the coating process. Furthermore, the Fe concentration evolution rather than Zn and Al in each layer was analysed, which was often observed some typical features in the open published literatures, but rarely been discussed. Based on the microstructure analyses of as-prepared coating, combining the results of the present study and of the literatures, the evolution mechanism of Zn-Al co-deposited coating prepared on low carbon steel by pack cementation was modelled and analysed from the perspective of gas-solid transition and the diffusion evolution in detail, hopefully, contributing to have a profound comprehension about the coating growth behaviour. Moreover, the corrosion resistance of as-received coatings was evaluated, which is also suitable for understanding the corrosion application of such a coating.

**Microstructure evolution of a Zn-Al coating co-deposited on
low-carbon steel by pack cementation**

Qi Xue, Cai yuan Sun, Jia Yan Yu, Ling Huang, Jun Wei, Jin Zhang*

School of Materials Science and Engineering, Southwest Petroleum
University, 610500 Chengdu, PR China

* Corresponding author

Tel: 13550217265; fax: +86 -28-83037406.

E-mail address: jzhang@swpu.edu.cn

Microstructure evolution of a Zn–Al coating co-deposited on low-carbon steel by pack cementation

Abstract: In this study, Zn–Al coatings were co-deposited on AISI 1020 steel by pack cementation. The as-prepared coatings were characterised by scanning electron microscopy, energy–dispersive x–ray spectroscopy, and x–ray diffraction. The evolution mechanism of the coating was modelled and analysed in detail. Furthermore, the corrosion resistance of the as-received coatings was investigated by a potentiodynamic polarisation test in a 3.5% NaCl solution. We observed that the relatively loose and porous structure of those coatings was a function of the Al content in the packed powders. The regions with a natural porous structure evidently increase with an increase in Al concentration. The Zn-rich layer was formed because of the dominant inward diffusion of Zn with a small diffusion of Fe in the substrate. Thus, the Zn-rich layer/substrate interface moved into the ferrous substrate. As the reaction continued, the deposition of Al dominated. The interdiffusion of Al and Zn in the Zn-rich layer and the diffusion of Fe into the Zn-rich layer towards the Al-rich layer led to the nucleation and growth of the Fe–Al phases and the consumption of the Zn-rich layer. As a consequence, the Al-rich layer/Zn-rich layer interface moved inside the Zn-rich layer. At higher deposition temperatures, when the heat was released because of the Fe–Al phase formation, the evaporation of Zn resulted in void formation in the Al-rich layer. The potentiodynamic polarisation test results show that both Zn and Zn–Al coatings significantly enhance the corrosion resistance of a ferrous substrate, but Zn–Al coatings seem to be more efficient.

Key words: corrosion resistance; evolution mechanism; microstructure; pack cementation; Zn–Al co–deposited coating

1. Introduction

Many features of Zinc make it very suitable for use as a protective coating for ferrous substrates. For example, zinc coatings can react with atmospheric compounds (O_2 , CO_2 , and H_2O) to form dense, adherent films over the coating surface. The corrosion rate of such films is considerably lower than that of ferrous materials [1, 2]. Because zinc's corrosion potential is lower than that of ferrous material, zinc coatings can also provide sacrificial cathode corrosion protection. Consequently, zinc coatings are widely used for corrosion control in the construction, automobile, utility and appliance industries [3–5].

However, the corrosion resistance of a pure Zn coating on steel is not satisfactory under severe atmospheric conditions or corrosive aqueous solutions [6, 7]. To increase the corrosion resistance of Zn-coated steel, previous researchers have made great efforts to optimise the composition of the Zn coating. Many studies have demonstrated that the mechanical properties and corrosion resistance of the ferrous substrate could be enhanced by adding other elements to the pure Zn coating, such as Ni [8–10], Co [9], Cr [2, 11, 12], Mg [13, 14], Si [15], and Al [2, 3, 5, 15–20]. Zinc coatings alloyed with Al have been developed and widely applied. To combine the advantages of single Zn and Al coatings, in recent years such coatings have been proposed for magnesium and magnesium alloys [17–19] and carbon steel [20, 21] to

prolong the service life of work pieces.

Various methods have been used for depositing that coating, such as physical vapour deposition [21, 22], thermal spray [23], hot dipping [3, 24, 25], and pack cementation [2, 5, 20]. Among them, pack cementation possesses distinct advantages, such as simple equipment requirements, easy processing, and low cost, and it could be applied to components with a range of geometrical dimensions and complexities. More importantly, this technology is fairly environmentally friendly, because no toxic fumes emerge during the formation of the film [2, 26, 27].

Up to now, only a limited number of studies have been made on depositing a Zn–Al coating on carbon steel by pack cementation. Several authors have reported that this method yields a 2-layered structure. The outer layer has a high content of Al together with smaller amounts of Zn and Fe, and the inner layer consists of Zn, Fe, and a small amount of Al. Furthermore, the Fe–Zn layer was compact, but the Fe–Al layer was porous. The obtained coating could significantly promote the oxidation resistance and corrosion resistance of the ferrous substrate. The work carried out by Shen et al. [5] verified that the Zn–Al co-deposition process is chemical vapour deposition (CVD) induced by chemical activators. They point out that during the process, an Fe–Zn layer was formed first. Fe–Al phases then nucleated locally on the surface of the Fe–Zn layer. With continued reaction, a complete Fe–Al layer was formed and grew at the expense of the Fe–Zn layer.

Unfortunately, most published studies focus on cross-sectional analyses instead of surface morphologies. Furthermore, the analyses focus on the concentration evolution

of Zn and Al in each layer. Few detailed analyses have been carried out on the concentration evolution of Fe in each layer. However, because the formation of the Fe–Zn and Fe–Al phases is directly related to the Fe, its evolution is of prime importance for coating growth. It is not yet clear how to interpret the evolutionary process and mechanism of the formation of such a coating from the perspective of gas–solid transition and the view of diffusion evolution.

Because of the gaps in the available reference data, we systematically studied the microstructure, surface and cross-section morphology, and phase constituents of Zn–Al co–deposited coating on the surface of low–carbon steel by the pack cementation process, and also investigated the concentration evolution of Fe. We propose a simplified model for this coating growth on a low–carbon steel substrate based on the results of the present study and of the literature. Additionally, we did a potentiodynamic polarisation test to evaluate the corrosion behaviour of the as–received coatings.

2. Experimental procedure

2.1. Materials and preparation

As a substrate, we used commercial low carbon steel, AISI 1020 (0.186% C, 0.022% Cr, 0.017% Cu, 0.509% Mn, 0.002% Mo, 0.013% Ni, 0.003% P, 0.030% S, 0.106% Si, and the balance Fe in wt%). The sample size was $50 \times 15 \times 5$ mm. Before the deposition process, we grounded and polished the substrates with a series of SiC

emery papers down to 1200 grit. This was done to smooth the surface and remove its oxide layer and other contaminants. Then the substrates were ultrasonically cleaned in acetone, ethanol, and deionised water sequentially for 15 min.

2.2. Zn–Al co-deposition

A Zn–Al co-deposited coating was prepared by the pack cementation method. For the pack mixtures, we used Zn and Al powder, NH_4Cl halide salt, and alumina powder as the donor material, activator, and filler of the pack respectively. The formulations of the powder mixtures are summarised in Table 1. The substrates were then covered with the pack powders in a cylindrical alumina crucible sealed with alumina-based cement. The sealed crucible was cured for at least 1 h at room temperature and then further cured in a furnace for approximately 2 h at 80 °C in order to remove the remaining moisture. The furnace temperature was then raised to a final coating temperature of 460 °C for 4 h. The entire deposition process was carried out in the ambient atmosphere. After the heating period, the crucible remained in the furnace and was cooled to the ambient temperature. After that, the coated specimens were retrieved from the pack and cleaned in an ultrasonic alcohol bath to remove any residual powders on their surfaces.

2.3. Characterisation

We studied surface morphologies and cross sections of the specimens using an EVO MA15 scanning electron microscopy (SEM), with energy dispersive x-ray

spectroscopy (EDS) and the necessary software to do point/linear microanalysis of the coating. x-ray diffraction (XRD) using a DX-2000 tube and Cu-K α radiation was used to identify the phases formed in the coatings. A step-scan mode was used in the 2-Theta range of 10° to 80°.

2.4. Corrosion test

The corrosion resistances of coatings were assessed by measuring the potentiodynamic polarisation curves (polarisation measurements) in a 3.5 wt% NaCl solution at 20 °C using a CS350 electrochemical workstation. The working electrode was Zn-Al co-deposited on carbon steel. Pretreatments in ethanol and water were done before the testing, as described in the section 2.1. The active surface area was 15 mm \times 10 mm. The reference electrode was a saturated calomel electrode, and a platinum plate was used as the counter electrode. The polarisation measurement was done at a scanning rate of 1 mV/s in the range of -200 mV to +700 mV by comparison with the open circuit potential (OCP) after a steady OCP was reached. After the test, we examined the samples microscopically and analysed them to determine the structure and chemical composition of the corrosion areas.

3. Results and discussion

3.1 Surface morphology

Fig.1 shows the surface microstructure of the as-received coating and the top-view SEM observation of the Zn-Al co-deposited coatings with various Al contents at

460 °C for 4 h. Clearly, in the absence of Al, as shown in Fig. 1a, the SEM topography of the as-prepared coating shows some visible microcracks and a relatively smoother surface compared to that with 10% Al (Fig. 1b) and 20% Al (Fig. 1c). In the case of the 10% Al coating, as shown in Fig. 1b, it is evident that the surface of the coating comprises 2 typical surface regions, one of which has a light grey colour and the other a dark grey colour. Magnified morphologies of the 2 regions are also shown in Figs. 1d and 1e. As can be seen in the figures, the dark grey region is very compact and dense without any visible pinholes or microcracks. The results of the EDS analysis show that this type of region is rich in Zn, with a small amount of Al and Fe. In contrast, the light grey region exhibits a loose and relatively porous structure. Its EDS analysis results show that this region is rich in Al, with a small amount of Zn and Fe. These results indicate that the Al-rich zones were locally formed on the coating surface.

The Zn–Al co-deposited coating with 20% Al, shown in Fig. 1c shows a loose and highly porous structure as a whole, with voids in the range of 0.5 to 3 μ m but free from visible microcracks, which is similar to the light grey regions in Fig. 1b. This observation is in good agreement with earlier studies [2, 5, 20]; those researchers observed similar microstructure features from cross-sectional observations. Based on the observations above, we could conclude that the addition of Al leads to a relatively loose and porous structure of the Zn–Al co-deposited coating. Furthermore, with an increase in Al content in the packed powder, the zones with loose and porous structure would expand until covering the entire surface.

A possible explanation for this behaviour is the fact that Al reacts with the Zn-rich layer in the final stage of the coating growth; this will be discussed in detail in section 3.4. Because the deposition temperature (460 °C) is evidently higher than the melting point of Zn (419.5 °C), when Al replaces Zn in the Zn-rich layer, the resultant Zn metal evaporate, leaving voids in the Al-rich layer. With increasing amounts of Al, an increasing number of Al atoms displace Zn in the Zn-rich layer; thus, more areas with loose and porous structures would appear on the surface of the coating. It could be inferred that the porous-structure characteristic of such a coating is related not only to the deposition temperature and heating time but also to the overall pack composition. Moreover, such formed porous structure would be responsible for the mechanical properties and corrosion resistance of the Zn–Al co-deposited coating, which should be evaluated in further research.

Fig.2 shows the results of an in-depth study of the microstructure of the outermost layer. It also shows the magnified morphology and the Fe, Zn, and Al elemental distribution maps, measured by EDS, of the Zn–Al co-deposited coating with 20% Al at 460 °C for 4 h. Results from the EDS map scans show that the distribution of major elements in the outer layer is uniform. Moreover, the outermost surface of the coated layer is enriched with Fe and Al, whose concentration was significantly higher than that of Zn, showing that the outermost surface of the coating is certainly the Al-rich layer. Furthermore, as shown by the arrows in Fig. 2, there are some granular particles on the surface, which might be related to the nucleation and growth mechanisms of Fe–Al phases on the surface of the Zn-rich layer, which need to be studied further.

3.2. Cross-sectional SEM micrograph and EDS analysis

Fig.3a shows a SEM micrograph of a typical cross-section the Zn–Al co-deposited coating prepared on the 1020 steel at 460 °C for 4 h. It is clear that the as-prepared coating possessed a uniform thickness of approximately 45 μm and could be divided into 2 layers. The thicknesses of the outer and inner layers were approximately 5 and 40 μm respectively. Also taking into account the EDS analysis results from the coating surface to the core, clearly Al tends to be in the outer layer and Zn in the inner layer. Specifically, the amount of Al is much higher than that of Zn in the outer layer, which is consistent with the result displayed in Fig. 2, thus the outer layer could be called an Al-rich layer. Similarly, the concentration of Zn is apparently higher than that of Al in the inner layer, which could be labelled the Zn-rich layer.

This double-layer structure has been observed in other studies also, although the coating processes were different. A growth and evolution model of such a coating is proposed in section 3.4. Actually, those studies have reported that such a 2-layered structure could effectively enhance resistance to corrosion and high-temperature oxidation. However, it must be pointed out that there are still some differences among those studies, such as the total thickness of the as-prepared coating; the thicknesses of the Al-rich and Zn-rich layers; and the ratio of the Al-rich layer to the Zn-rich layer, which is close to 1:8 in our study, but 4:5 in [20] and 1:2 in [2]. Such differences may result from the experimental conditions (here, this refers to the substrate material, the formulation of the cementation powder, and the treatment temperature and duration, with or without a protective atmosphere).

In addition, as shown by the arrows in Fig. 3a, some cracks are in the Zn-rich layer. This phenomenon is common in zinc coatings prepared by the pack cementation process. A possible reason for the formation of cracks is the mismatch in the coefficient of thermal expansion between the Zn-rich layer and the Al-rich layer or between the Zn-rich layer and the substrate, or both, leading to tensile residual stress during the cooling process. Formation of microcracks among columnar grains could release the stress in the coating [26, 28]. In fact, the pack cementation process activated by halide salt involves gas-phase diffusion of the metallic halide vapours and solid-state diffusion between the deposited elements and the substrate, which leads to the nucleation and growth of the coating and the evolution of the interface. In such a complex process, this could be another cause of cracks during coating growth.

The published literature illustrates that the growth rate of the Zn and Zn–Al coatings deposited by the pack cementation process is relatively high, which might lead to the initiation and propagation of cracks as well. Certainly, the coating growth rate of that process is essentially associated with the reaction process and preparation conditions, such as the reaction temperature, the type of activator, and the addition of rare earth in the pack composition. How those factors affect the formation of cracks in Zn and Zn–Al coatings must to be studied further.

Fig. 3b shows the concentration profiles of major elements across the cross sections of the as-prepared coating. Table 2 summarises the EDS point analysis of the representative zones in the coating (marked A, B, C, and D in Fig. 3a). It is obvious that both Zn and Al were detected in the coating and the substrate, indicating the

occurrence of the co-deposition process. However, Al was found mainly in the outermost surface of the coated layer, and Zn beneath the top layer. The Al content was minor in both the Zn-rich layer and the substrate, likely because of the limited solubility of Al in the Fe–Zn phase and the α -Fe. Note that the Zn and Fe content at point B (the zone of the Zn-rich layer centre) is close to the δ phase, and at point C (the zone of the Zn-rich layer near the substrate) is close to the Γ phase, according to the Zn–Fe binary phase diagram [29].

We were surprised to find that the concentration of Fe was very high in the Al-rich layer and dropped abruptly at the interface between the Al-rich and Zn-rich layers; Fe concentration increased progressively from the interface between the Al-rich and Zn-rich layers and the matrix, which is a common phenomenon in previous studies, but rarely mentioned. This phenomenon could be regarded as more evidence that Al substitutes for Zn in the Zn-rich layer in the final stage of co-deposition. This phenomenon is also the direct reason that there is a certain amount of Zn besides Al in the outermost layer of the coating. In fact, because of Al's higher affinity to Fe than to Zn [30], the build-up of Al on the surface of the Zn-rich layer might result in the diffusion of Fe in the Zn-rich layer towards the Al-rich layer, leading to the nucleation and growth of the Fe–Al phases and the consumption of the Zn-rich layer.

Additionally, the interface between each layer shows an apparent interdiffusion character, confirming that metallurgical bonding was formed between each interface.

Furthermore, the Al concentration remained high across the Al-rich layer (Fig. 3b), but dropped abruptly to approximately zero at the interface between the Al-rich and

Zn-rich layers. In the case of Zn, a similar feature was observed at the Zn-rich-layer/substrate interface. This is a typical feature showing that the coating is formed via a reaction diffusion mechanism, leading to the formation of compounds.

The O concentration evolution is another important factor that must be taken into consideration, because the entire deposition process was carried out in the ambient atmosphere. As is shown in Fig.3b, O was found in only the outermost surface of the coated Al-rich layer, and may have come from oxygen remaining between the powder grains of the pack mixture. Furthermore, the O concentration dropped abruptly to approximately zero at the interface between the Al-rich layer and the Zn-rich layer, implying that the absorption of O was accompanied by the formation of the Al-rich layer, which might be associated with the pressure evolution during this stage. This stage is discussed in the section 3.4. On the whole, however, the oxidation of the as-obtained coating was mild, as illustrated in Table 2 and Fig. 3b, which might be attributed to both the treatment temperature, which was low relative to that of many other pack cementation processes [26, 27], and to the effect of the sealing treatment.

3.3. Phase identification

Fig. 4 illustrates the XRD patterns of the Zn–Al co-deposited coating with 20% Al on low-carbon steel at 460 °C for 4 h. The results indicate that in the as-received coating there were AlFe (PCPDF 65-3201), $\text{Fe}_2\text{Al}_5\text{Zn}_{0.4}$ (PCPDF 49-1381), and $\text{FeZn}_{10.98}$ (PCPDF 45-1184) phases. The details of region A in Fig. 4a are shown in Fig. 4b; each peak line from the $\text{FeZn}_{10.98}$ in a high-diffraction angle region consists

of some closely overlapped small peaks, indicating the existence of more than one phase. We compared these weak diffraction patterns and the Joint Committee on Powder Diffraction Standards (JCPDS) files, and found that the patterns belong to $\text{Fe}_{11}\text{Zn}_{40}$ (PCPDF 65-5438). This phase was traced with EDS analysis as shown in Fig. 3b. This finding is consistent with the observation of Chaliampalias et al. [2]. Conversely, He et al. [20] reported that the outer layer was composed mainly of Fe_2Al_5 and the FeAl intermetallics phase, and the diffraction peaks of $\text{Fe}_{11}\text{Zn}_{40}$ could not be found. This may be because that the outermost layer of the as-prepared coating was thicker than those in our study and in [2].

Combined with the EDS analysis as shown in Fig. 3 and the evolution process of the as-prepared coating [4, 20], which is discussed in the section 3.4, it is reasonable to deduce that the treated samples were composed of phase constitution in the following sequence from the outermost surface towards the core: $\text{AlFe}+\text{Fe}_2\text{Al}_5\text{Zn}_{0.4}$, $\text{FeZn}_{10.98}$, and $\text{Fe}_{11}\text{Zn}_{40}$.

3.4. Evolution of the Zn–Al co-deposited coating

Combining the results of both the present study and the literature, and based on the above discussion about the surface morphology and cross-sectional microstructure as well as the phase constituents of the as-prepared coating, we propose a simplified model for the evolution of Zn–Al co-deposited coating growth on a low-carbon steel substrate.

It is commonly accepted that pack cementation is effectively an in situ chemical

vapour deposition process. During the coating process, the entire pack is heated to an appropriate temperature at which the halide salt activator reacts with the depositing elements to form a series of halide vapours; the vapours then pass through the porous pack to reach the substrate surface due to the chemical potential gradient between the depositing element and the substrate [5, 26, 31–33]. Specifically, under our experimental condition, NH_4Cl would decompose to be NH_3 and HCl with the gradual rise in temperature; then the HCl would react with the Zn and the Al to form a series of chloride vapours containing Zn or Al . Among those chloride vapours, ZnCl_2 takes charge of transporting and depositing Zn and AlCl_3 for Al , as shown in Fig. 5a.

Furthermore, note that the reaction between the Zn and the Fe in the substrate is an exothermic reaction [23], leading to the further reaction between Fe and Zn and Al .

The work carried out by Chaliampalias et al. indicates that the effect of Al is limited for the structure change of the Zn coating. The Al is distributed mainly on the surface of the specimens, forming an additional layer, that is to say it is the primary zincing process in the initial stages of coating growth. Vourlias [34] pointed out that the zinc coating is formed through the diffusion of zinc in the ferrous substrate (inward diffusion) ; in other words, when Zn reacts with Fe , Zn atoms are the predominant moving species. The chemical potential gradient of the depositing element (Zn and Al) drives Zn and Al atoms to diffuse towards the substrate.

A series of studies indicates that co-deposition of 2 or more elements by the halide activated pack cementation method is especially difficult because the halide vapour pressures, including different depositing elements, normally differ greatly, and are a

direct factor contributing to the multilayer structure [31, 33, 35]. Interestingly, a similar multilayer structure was obtained in our study. Clearly, the treatment temperature (460 °C) is much closer to the temperature for the Zn coating growth (in the range of 350 °C to 450 °C) and is lower than the temperature for the aluminum coating (>550 °C) [36, 37]. Therefore, we can deduce that the partial pressure of chloride vapours, which take charge of transporting and depositing Zn, was higher than that of Al in the initial stage under our experimental conditions. As a consequence, Zn reacted with Fe in the ferrous substrate preferentially, forming the Fe-Zn compounds and creating the Zn-rich layer gradually. It is worth mentioning that when the reaction diffusion between Zn and the ferrous substrate occurred, the concentration of Fe atoms in the surface layer of the substrate continued to decrease, which also formed the driving force leading to the Fe atoms diffusing towards the subsurface of the ferrous substrate; this process, however, was not the primary process. Therefore, the interface between the Zn-rich layer and the substrate showed mutual diffusion characteristics, which has been shown in the EDS analysis. In addition, as the growth time increased, the Zn-rich layer/substrate interface moved inside the ferrous substrate from the perspective of growth kinetics, as shown in Figs. 5b and 5c.

As the Zn in the cementation powder was consumed, the partial pressure of chloride vapours, which take charge of transporting and depositing Zn would theoretically suffer continual decline. Conversely, as for Al, the partial pressure of the corresponding chloride vapours exhibited the opposite variation trend and increased gradually. If the vapour pressures of the 2 vapour species are within 1 to 2 orders of

magnitude, then the co-deposition of 2 elements will be realized. As the reaction continues, the partial pressure of chloride vapours, which take charge of transporting and depositing Al, would increase considerably; then, the deposition of Al would dominate and the concentration of Al would build-up markedly. At this time, the Fe–Al phases crystallised on the surface of the Zn-rich layer, as shown in Fig. 5d. Such a process may be mainly due to a higher affinity of Al towards Fe than towards Zn.

The build-up of Al on the surface of the Zn-rich layer might result in substitutional diffusion between Al and Zn in the Zn-rich layer and the diffusion of Fe in the Zn-rich layer towards the Al-rich layer, leading to the nucleation and growth of the Fe–Al phases and the consumption of the Zn-rich layer. Therefore, we suggest that the growth of the Al-rich layer was at the expense of the Zn-rich layer.

The Al-rich layer/Zn-rich layer interface moves inside the Zn-rich layer as the reaction continues. The Fe–Al phases appear earlier on top of the Zn-rich layer as the weight ratio of Al powders to Zn powders in the pack is increased [5]. Furthermore, the larger the ratio of Al powders to Zn powders in the packed powder, the more regions enriched in Al appear on the outermost layer, which is discussed in the section 3.1.

It is also worth noting that because the depositing temperature (460 °C) was evidently higher than the melting point of Zn (419.5 °C), when Al displaces Zn in the Zn-rich layer, the resultant Zn atoms would evaporate. Moreover, the diffusion of Fe in the Zn-rich layer towards the Al-rich layer may speed the consumption of the

Zn-rich layer and contribute to the evaporation of Zn atoms. In addition, the formation of Fe–Al compounds is highly exothermic [24], and the heat released as the phase forms locally may also speed up the evaporation process of Zn atoms, leaving voids in the Al-rich layer, as shown in Fig.5e. To sum up, the entire coating process is effectively controlled by the solid-state diffusion growth of the coating layers and could be defined as a reaction diffusion process.

3.5. Corrosion behaviour

Fig. 6 shows the potentiodynamic polarisation curves for the Zn and Zn–Al coatings measured in 3.5% NaCl solution. The polarisation curve of the uncoated substrate is presented also, as a reference. Table 3 summarises the electrochemical corrosion parameters obtained by Tafel polarisation curves. The values of corrosion potential (E_{corr}) for the Zn and Zn–Al coatings were clearly lower than those of the bare substrate. A marked decrease of E_{corr} for Zn and Zn–Al coatings may have resulted from the existence of Zn [2, 3]. Consequently, the relatively lower corrosion potential indicates that such coatings could provide sacrificial cathodic corrosion protection for the base material. Furthermore, the E_{corr} for Zn–Al coatings were considerably more positive than for the Zn coating, which could be explained by the effect of Al on the structure of the coatings. Moreover, the E_{corr} for Zn–Al coatings with different Al content were extremely close, indicating that the E_{corr} was more likely associated with the composition than with the surface morphologies of the as-obtained coatings.

Corrosion current density (I_{corr}) is another important parameter for determining the kinetics of the corrosion reaction, and it is normally proportional to the corrosion rate. As can be seen in Table 3, evidently the corrosion rates increased in the following sequence: Zn–Al coating (10% Al) < Zn–Al coating (20% Al) < Zn coating < bare substrate, showing that both the Zn and Zn–Al coatings with different Al content could markedly enhance the corrosion resistance of the ferrous substrate. The Zn–Al coatings could improve the corrosion resistance relatively more effectively, which could be attributed to their duplex structure.

To better illustrate the corrosion behaviour of such a coating, we created the Figs. 7a–b and 7c–d, which show surface images of the bare substrate and the Zn–Al coating (20% Al) at a lower and higher magnification respectively after the polarisation test. As is shown in Figs. 7a and 7b, with an inhomogeneous dissolution the results clearly show localised corrosion, rather than general corrosion, of the bare substrate. By comparison, as can be seen in Figs. 7c and 7d, in the case of Zn–Al coating (20% Al), there were 2 typical morphological features. One, the area marked B in Fig. 7d, exhibited a laminar and/or needle-like structural characteristic. The corresponding EDS results prove that this zone is rich in Zn but lacks Al. Compared with the original EDS map results of the coating shown in Fig. 2, it is not difficult to infer that this zone on the top surface of the Al-rich layer had suffered a catastrophe. The other area, marked A in Fig. 7d, displays a relatively compact and dense surface structure. The corresponding EDS results confirm that this zone is also rich in Zn but its content is lower than it is for region B. In comparison, a small amount of Al was

detected in this area but its concentration is evidently lower than the initial Al-rich layer on the outermost surface as well, which indirectly shows that this region on the surface of the Al-rich layer had partially broken down.

Furthermore, the concentration of Fe and Al showed the same tendency to decrease when compared with the initial outermost layer. This is because the outermost Al-rich layer was composed mainly of the Fe–Al phases. With the breakdown of the Al-rich layer in the corrosion medium, the content of Fe and Al on the surface decreased simultaneously. Additionally, O and Cl were detected in both areas, which may be associated with corrosion products [38]. These corrosion products might be responsible for the different morphologies of the A and B areas in Fig. 7d.

Aluminised coatings tend to form a passive film, indicating that the Al-rich layer might theoretically provide more resistance to corrosion. However, the porous structure of the as-received coating allows the free flow of the liquid corrosive media and more contact area with the inner Zn-rich layer. The reaction between the corrosive media and the Zn-rich layer could lead to spalling of the Al-rich layer, partially due to adhesion failure along the Al-rich layer/Zn-rich layer interface, the region marked B in Fig. 7d. Fortunately, the inner Zn-rich layer could act as a barrier to block a direct path between a corrosive environment and the substrate. Moreover, the secondary barrier action of the zinc corrosion products and the cathodic protection of zinc could effectively enhance the corrosion resistance of the base material [3, 38].

4. Conclusions

In the present work, we investigated the microstructure and the evolution mechanism of a Zn–Al co-deposited coating on the surface of low-carbon steel by the pack cementation process. The main findings are listed as follows.

The relatively loose and porous structure of the Zn–Al co-deposited coating was governed by the addition of Al. With an increase of the Al content in the packed powder, the natural porous structure became increasingly obvious. The obtained coating had a double-layer structure. The outermost layer was Al- rich layer, containing a high concentration of Fe with a small amount of Zn. The inner layer was Zn- rich, composed of Fe–Zn phases.

Because the treatment temperature was much closer to the temperature for the zinc coating growth, the Zn-rich layer formed preferentially. In this process, the inward diffusion of Zn dominated with a small diffusion of Fe in the substrate, while the Zn-rich layer/substrate interface moved inside the ferrous substrate. As the reaction continued, the partial pressure of chloride vapours, which take charge of transporting and depositing Al, increased considerably, and then the deposition of Al dominated and the concentration of Al built up markedly. Because of a higher affinity of Al towards Fe than towards Zn, the build-up of Al on the surface of the Zn-rich layer might have resulted in replacement behaviour between Al and Zn in the Zn-rich layer and a substantial diffusion of Fe in the Zn-rich layer towards the Al-rich layer, this could have contributed to the formation and growth of the Fe–Al phases and the consumption of the Zn-rich layer. As a consequence, the Al-rich layer/Zn-rich layer

interface moved inside the Zn-rich layer as the reaction continued.

Because the deposition temperature was evidently higher than the melting point of Zn, the formation of Fe–Al compounds was highly exothermic, and the Fe in the Zn-rich layer diffused towards the Al-rich layer, the evaporation process of resultant Zn atoms would have been enhanced, leaving voids in the Al-rich layer.

The corrosion current density (I_{corr}) increased in the following sequence: Zn–Al coatings (10% Al: $7.1900 \times 10^{-6} \text{ Acm}^{-2}$; 20% Al: $8.2472 \times 10^{-6} \text{ Acm}^{-2}$) < Zn coating ($9.1376 \times 10^{-6} \text{ Acm}^{-2}$) < bare substrate ($2.7655 \times 10^{-5} \text{ Acm}^{-2}$), showing that both the Zn and Zn–Al coatings could greatly enhance the corrosion resistance of the ferrous substrate. Moreover, better corrosion resistance was obtained by the Zn–Al coatings than by the Zn coating.

Acknowledgments

This work was supported by the Undergraduate Innovation and Entrepreneurship Programme in Si Chuan province (No. KSZ14122); the Youth science and technology innovation team of electrochemistry for energy materials (Southwest Petroleum University, No.2015CXTD04); and the Key Lab of Material of Oil and Gas Field (X151516KCL02).

References

- [1] G. Vourlias, N. Pistofidis, D. Chaliampalias, E. Pavlidou, G. Stergioudis, E.K. Polychroniadis, D. Tsipas, Zinc deposition with pack cementation on low carbon steel

- substrates, *J. Alloys Compd.* 416 (2006) 125–130.
- [2] D. Chaliampalias, M. Papazoglou, S. Tsipas, E. Pavlidou, S. Skolianos, G. Stergioudis, G. Vourlias, The effect of Al and Cr additions on pack cementation zinc coatings, *Appl. Surf. Sci.* 256 (2010) 3618–3623.
- [3] H.C. Shih, J.W. Hsu, C.N. Sun, S.C. Chung, The lifetime assessment of hot-dip 5% Al-Zn coatings in chloride environments, *Surf. Coat. Technol.* 150 (2002) 70–75.
- [4] N. Pistofidis, G. Vourlias, D. Chaliampalias, K. Chrysafis, G. Stergioudis, E.K. Polychroniadis, On the mechanism of formation of zinc pack coatings, *J. Alloys Compd.* 407 (2006) 221–225.
- [5] T.H. Shen, C.Y. Tsai, C.S. Lin, *Surf. Coat. Technol.* [http://dx.doi:10.1016/j.surfcoat.2016.02.040](http://dx.doi.org/10.1016/j.surfcoat.2016.02.040)
- [6] P. Volovitch, C. Allely, K. Ogle, Understanding corrosion via corrosion product characterization: I. Case study of the role of Mg alloying in Zn-Mg coating on steel, *Corros. Sci.* 51 (2009) 1251–1262.
- [7] T. Prosek, A. Nazarov, U. Bexell, D. Thierry, J. Serak, Corrosion mechanism of model zinc-magnesium alloys in atmospheric conditions, *Corros. Sci.* 50 (2008) 2216–2231.
- [8] C. Bowden, A. Matthews, A study of the corrosion properties of PVD Zn-Ni coatings, *Surf. Coat. Technol.* 76 (1995) 508–515.
- [9] J. Giridhar, W.J. van Ooij, Study of Zn-Ni and Zn-Co alloy coatings electrodeposited on steel strips I: Alloy electrodeposition and adhesion of coatings to natural rubber compounds, *Surf. Coat. Technol.* 52 (1992) 17–30.

- [10] S.A. Ataie, A. Zakeri, Improving tribological properties of (Zn-Ni)/nano Al_2O_3 composite coatings produced by ultrasonic assisted pulse plating, *J. Alloys Compd.* 674 (2016) 315–322.
- [11] L. Guzman, M. Adami, W. Gissler, S. Klose, S. D. Rossi, Vapour deposited Zn-Cr Alloy coatings for enhanced manufacturing and corrosion resistance of steel sheets, *Surf. Coat. Technol.* 125 (2000) 218–222.
- [12] T. Boiadjieva, L. Mirkova, H. Kronberger, T. Steck, M. Monev, Hydrogen permeation through steel electroplated with Zn or Zn-Cr coatings, *Electrochim. Acta.* 114 (2013) 790–798.
- [13] N.C. Hosking, M.A. Ström, P.H. Shipway, C.D. Rudd, Corrosion resistance of zinc-magnesium coated steel, *Corros. Sci.* 49 (2007) 3669–3695.
- [14] J.H. La, S.Y. Lee, S.J Hong, Synthesis of Zn-Mg coatings using unbalanced magnetron sputtering and their corrosion resistance, *Surf. Coat. Technol.* 259 (2014) 56–61.
- [15] H.Q. Yang, Z.J. Yao, D.B. Wei, W.B. Zhou, G.X. Yin, L.X. Feng, Anticorrosion of thermal sprayed Al-Zn-Si coating in simulated marine environments, *Surf. Eng.* 30 (2014) 801–805.
- [16] O.S.I. Fayomi, A.P.I. Popoola, V.S. Aigbodion, Investigation on microstructural, anti-corrosion and mechanical properties of doped Zn-Al- SnO_2 metal matrix composite coating on mild steel, *J. Alloys Compd.* 623 (2015) 328–334.
- [17] S.J. Pan, W.T. Tsai, J.K. Chang, I.W. Sun, Co-deposition of Al-Zn on AZ91D magnesium alloy in AlCl_3 -1-ethyl-3-methylimidazolium chloride ionic liquid,

Electrochim. Acta.55 (2010) 2158–2162.

[18] M. Zhou, X.L. Pang, L. Wei, K.W.Gao, Insitu grown superhydrophobic Zn-Al layered double hydroxides films on magnesium alloy to improve corrosion properties, Appl. Surf. Sci. 337 (2015) 172–177.

[19] J. Hirmke, M.X. Zhang, D.H. StJohn, Surface alloying of AZ91E alloy by Al-Zn packed powder diffusion coating, Surf. Coat. Technol. 206 (2011) 425–433.

[20] Y.D. He, D.Z. Li, D.R. Wang, Z.E. Zhang, H.B. Qi, W. Gao, Corrosion resistance of Zn-Al co-cementation coatings on carbon steels, Mater. Lett. 56 (2002) 554–559.

[21] M.A. Baker, W. Gissler, S. Klose, M. Trampert, F. Weber, Morphologies and corrosion properties of PVD Zn-Al coatings, Surf. Coat. Technol. 125 (2000) 207–211.

[22] A. Perez, A. Billard, C. Rébéré, C. Berziou, S. Touzain, J. Creus, Influence of metallurgical states on the corrosion behaviour of Al-Zn PVD coatings in saline solution, Corros. Sci. 74 (2013) 240–249.

[23] Y. Wang, T.M. Zhang, W.M. Zhao, X.Y. Tang, Sealing Treatment of Aluminum Coating on S235 Steel with Thermal Diffusion of Zinc, J. Therm. Spray Technol. 24 (2015) 1052–1059.

[24] Z.W. Chen, J.T. Gregory, R.M. Sharp, Intermetallic phases formed during hot dipping of low carbon steel in a Zn-5 pct Al melt at 450 °C, Metall. Trans. A. 23 (1992) 2393–2400.

[25] Q. Luo, Q. Li, J.Y. Zhang, H.S. Lu, L. Li, K.C. Chou, Microstructural evolution and oxidation behavior of hot-dip 55 wt.% Al-Zn-Si coated steels, J. Alloys Compd.

646 (2015) 843–851.

[26] Y.Q. Qiao, X.P. Guo, Formation of Cr-modified silicide coatings on a Ti-Nb-Si based ultrahigh-temperature alloy by pack cementation process, *Appl. Surf. Sci.* 256 (2010) 7462–7471.

[27] D. Stathokostopoulos, D. Chaliampalias, E.C. Stefanaki, G. Polymeris, E. Pavlidou, K. Chrissafis, E. Hatzikraniotis, K.M. Paraskevopoulos, G. Vourlias, Structure, morphology and electrical properties of Mg₂Si layers deposited by pack cementation, *Appl. Surf. Sci.* 285 (2013) 417–424.

[28] N. Pistofidis, G. Vourlias, D. Chaliampalias, E. Pavlidou, G. Stergioudis, E.K. Polychroniadis, Comparative study of the corrosion behavior of zinc coatings deposited on low carbon steel substrates, *Surf. Interface Anal.* 38 (2006) 252–254.

[29] N. Pistofidis, G. Vourlias, D. Chaliampalias, E. Pavlidou, K. Chrissafis, G. Stergioudis, E. Polychroniadis, D. Tsipas, DSC study of the deposition reactions of zinc pack coatings up to 550 °C, *J. Therm. Anal. Calorim.* 84 (2006) 191–194.

[30] J. Liu, S.C. Jiang, Y. Shi, C. Ni, J.K. Chen, G.Z. Huang, Effects of zinc on the laser welding of an aluminum alloy and galvanized steel, *J. Mater. Process. Technol.* 224 (2015) 49–59.

[31] Z.D. Xiang, P.K. Datta, Pack aluminisation of low alloy steels at temperatures below 700 °C, *Surf. Coat. Technol.* 184 (2004) 108–115.

[32] Z.L. Zhan, Y.D. He, D.R. Wang, W. Gao, Low-temperature processing of Fe-Al intermetallic coatings assisted by ball milling, *Intermetallics.* 14 (2006) 75–81.

[33] M. Qiao, C.G. Zhou, Co-deposition of Co-Al-Y on nickel base superalloys by

pack cementation process, *Corros. Sci.* 75 (2013) 454–460.

[34] G. Vourlias, N. Pistofidis, K. Chrissafis, E. Pavlidou, G. Stergioudis, Mechanism and kinetics of the formation of zinc pack coatings, *J. Therm. Anal. Calorim.* 91 (2008) 497–501.

[35] Y.Q. Qiao, Z. Shen, X.P. Guo, Co-deposition of Si and B to form oxidation-resistant coatings on an Nb-Ti-Si based ultrahigh temperature alloy by pack cementation technique, *Corros. Sci.* 93 (2015) 126–137.

[36] K.R. Karimov, A.I. Anfinogenov, Y.B. Chernov, V.V. Chebykin, A.A. Pankratov, B.D. Antonov, Thermal diffusion zincing/aluminizing of steels and alloys under mechanical activation of sample surfaces, *Russ. J. Appl. Chem.* 83 (2010) 1804–1810.

[37] N. Kandasamy, L.L. Seigle, F.J. Pennisi, The kinetics of gas transport in halide-activated aluminizing packs, *Thin Solid Films.* 84 (1981) 17–27.

[38] A. Perez, A. Billard, C. Rébéré, C. Berziou, S. Touzain, J. Creus, Influence of metallurgical states on the corrosion behaviour of Al-Zn PVD coatings in saline solution, *Corros. Sci.* 74 (2013) 240–249.

Table and Figure Captions

Table 1. Chemical formulations of the deposition pack powders.

Table 2. EDS analysis of representative zones shown in Fig. 3.

Table 3. Results of the potentiodynamic polarization test.

Fig. 1. Top view SEM images of Zn–Al co-deposited coating with various Al contents. (a) 0 wt% , (b)10 wt% , (c)20 wt % at 460°C for 4 h , (d) and (e) are the representative regions in (b).

Fig. 2. EDS map of the Zn–Al co-deposited coating with 20% Al at 460 °C for 4 h.

Fig. 3. Zn–Al co-deposited coating at 460 °C for 4 h. (a) SEM cross-sectional image. (b) EDS analysis.

Fig. 4. XRD patterns of the Zn–Al co-deposited coating with 20% Al on low carbon steel at 460 °C for 4 h. (a) Region A is within the blue dashed line. (b) Details of region A.

Fig. 5. Schematic illustration of the evolution process of the Zn–Al co-deposited coating on low-carbon steel at 460 °C by the pack cementation process. (a) ZnCl_2 transporting and depositing Zn and AlCl_3 for Al. (b) and (c) Zn rich layer/substrate interface moving inside the ferrous substrate. (d) Fe–Al phases crystallising on the surface of the Zn-rich layer. (e) Evaporation process of Zn atoms leaving voids in the Al-rich layer.

Fig. 6. Typical potential polarization curves of the Zn and Zn–Al coatings

measured in a 3.5% NaCl solution. The curve of the uncoated substrate is shown as a reference.

Fig. 7. The surface images of the bare substrate (a-b) and the Zn–Al coating (20% Al) (c-d) at a lower and higher magnification respectively after the polarisation test.

Certificate of translation

		<h3>EDITORIAL CERTIFICATE</h3>		
<p>This document certifies that the manuscript listed below was edited for proper English language writing by one or more qualified native-English academic editors employed under the administration of the SmartStudy Education and Technology Group.</p>				
Affiliation	SOUTHWEST PETROLEUM UNIVERSITY	Date Issued	December 5th, 2016	
Reference No.	Manuscript Title	Word Count	Author	Contact
2176	Microstructure evolution of a Zn-Al coating co-deposited on low-carbon steel by pack cementation	5859	Jin Zhang	Tel: 13550217265; fax: +86 -28-83037406. E-mail: jzhang@swpu.edu.cn
<p>Smart Study Education and Technology Group</p>				
<p>December 14th, 2016</p>				
<p>Neither the research content nor the author's explicit intentions were in any way deliberately altered during the editing process. The English-language content of documents receiving this certification have been reviewed for and should be ready for publication internationally. However, the author of the document noted above reserves the right to accept or reject any suggestions and/or changes advised by the editor. If you have any questions or concerns regarding the aforementioned, edited document, please contact SmartStudy at xxx@innobuddy.com.</p>				

Table 1. Chemical formulations of the deposition pack powders

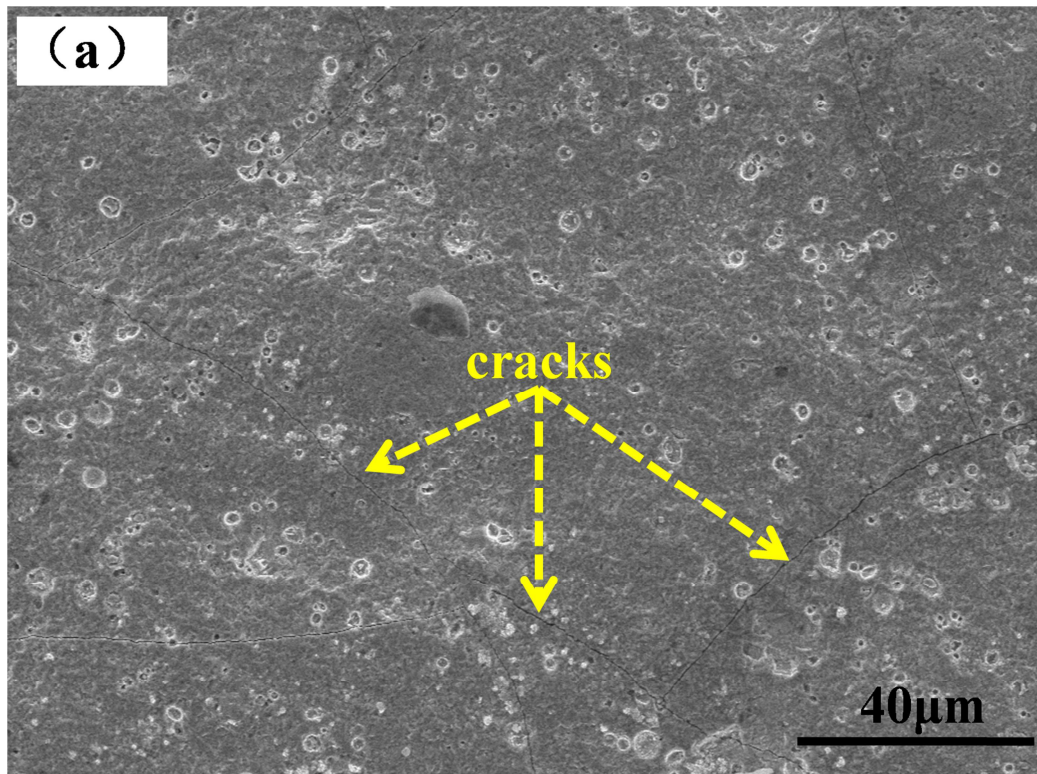
Pack	Zn	Al	NH ₄ Cl	Al ₂ O ₃
Zn-Al pack (wt.%)	50	0/10/20	2	Bal.

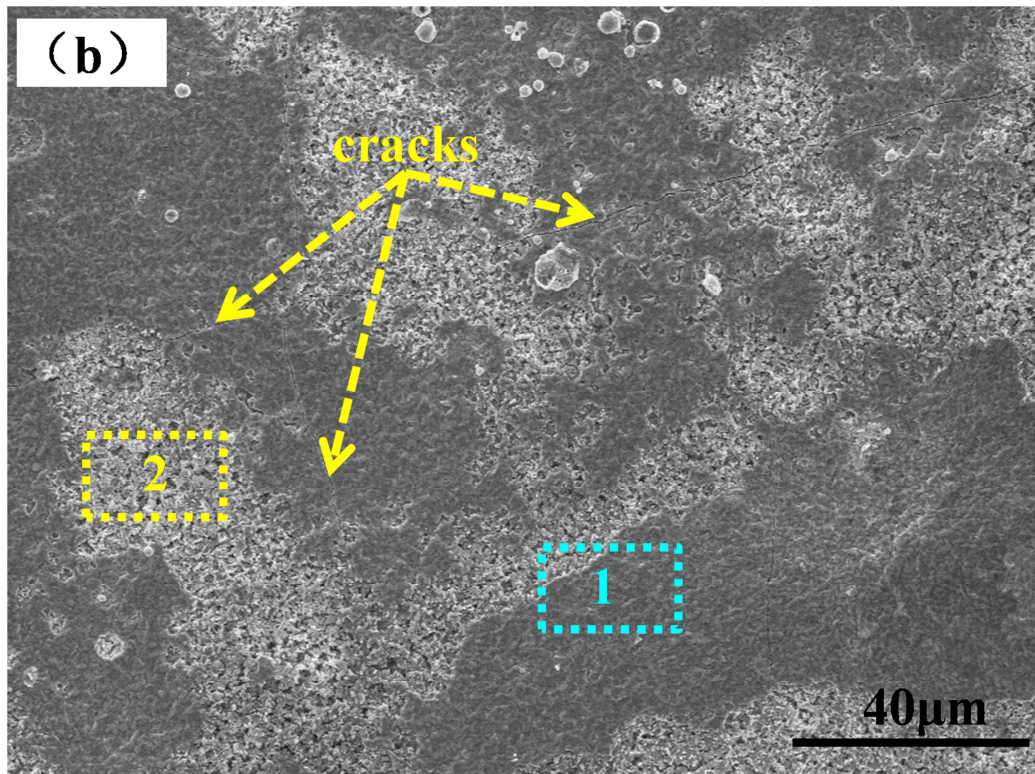
Table 2. EDS analysis of representative zones shown in Fig. 3a

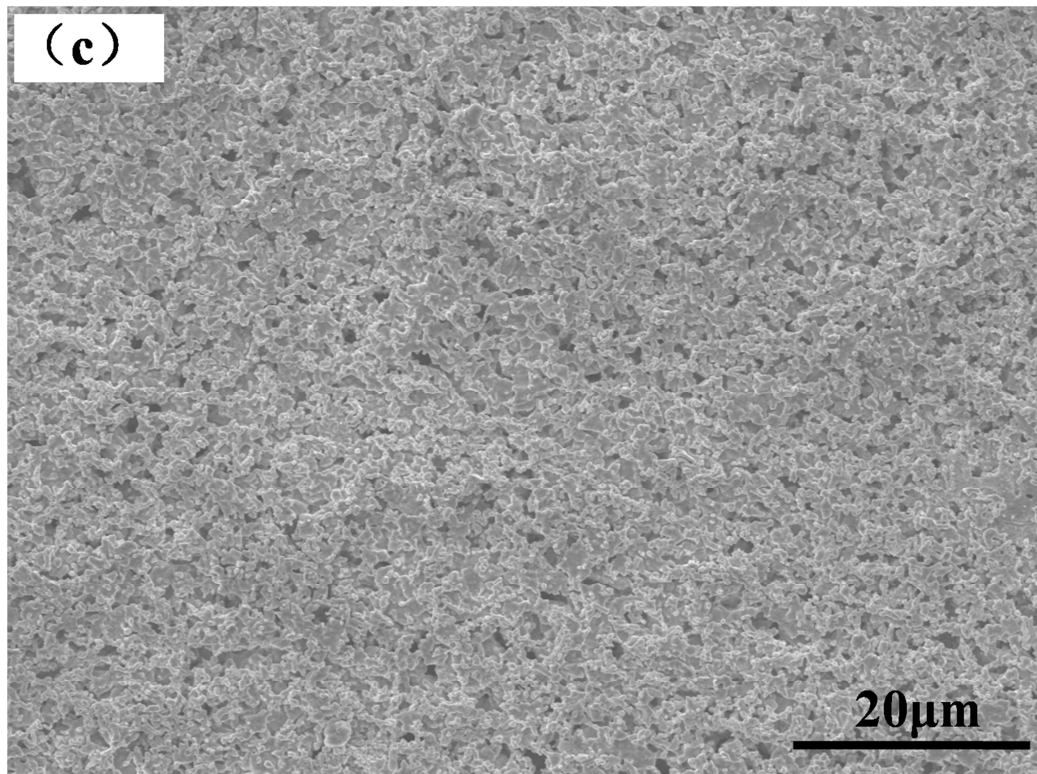
Position	Analysis zone	x(Al)/%	x(Zn)/%	x(Fe)/%	x(O)/%
A	Al-rich layer	28.66	1.17	69.16	1.01
B	Zn-rich layer (center)	0.26	87.34	12.22	0.18
C	Zn -rich layer (near substrate)	0.06	76.52	23.13	0.29
D	Substrate	0.08	0.44	99.47	0.01

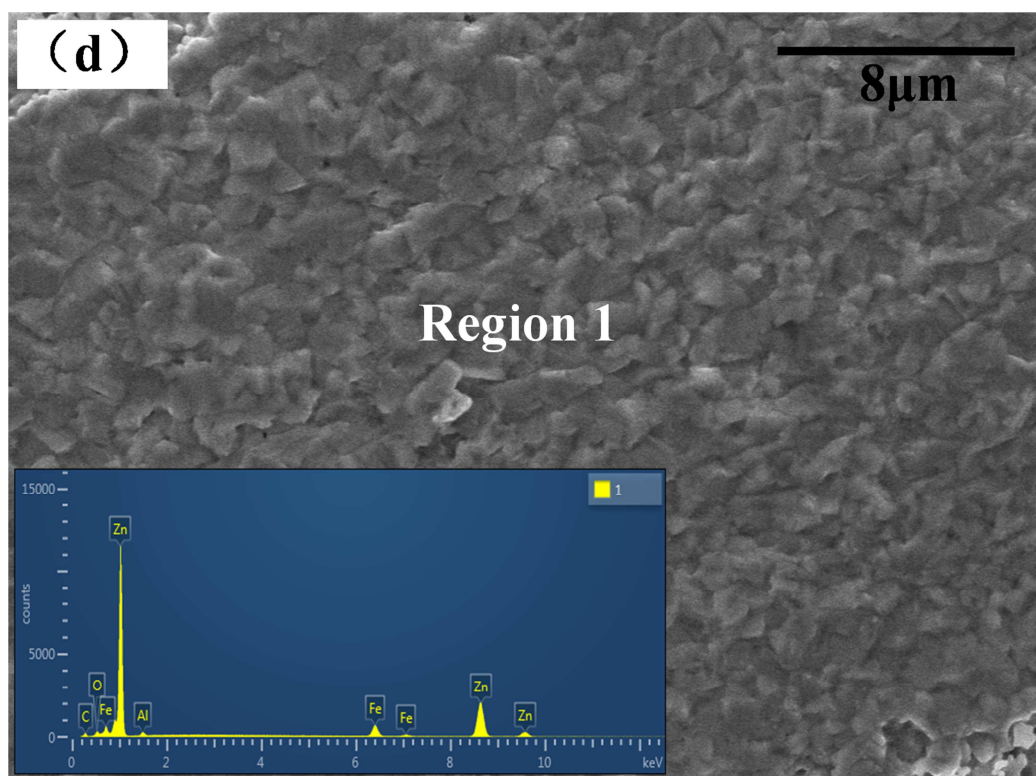
Table 3. Results of the potentiodynamic polarization test

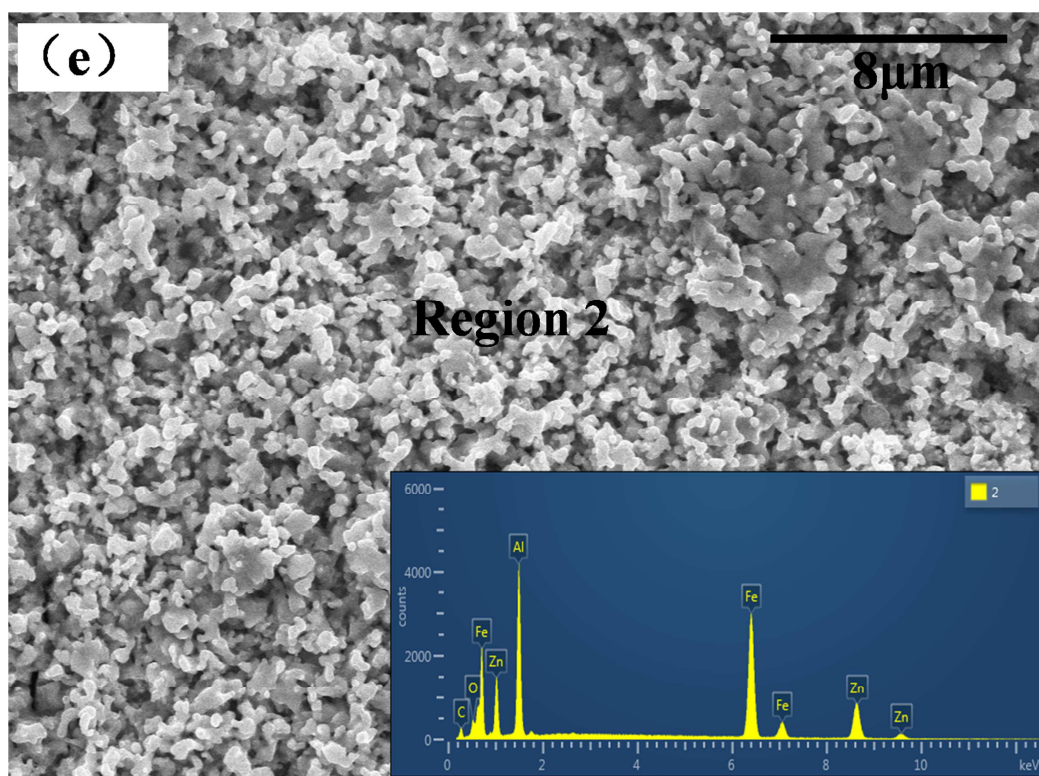
Specimens	Parameters	
	$I_{\text{corr}}(\text{Acm}^{-2})$	$E_{\text{corr}}(\text{V})$
Bare substrate	$2.7655 \times 10^{-5} \pm 0.0459 \times 10^{-5}$	-0.64947 ± 0.00346
Zn coating	$9.1376 \times 10^{-6} \pm 0.1190 \times 10^{-6}$	-0.99424 ± 0.00284
Zn-Al coating (10% Al)	$7.1900 \times 10^{-6} \pm 0.1976 \times 10^{-6}$	-0.88141 ± 0.00170
Zn-Al coating (20% Al)	$8.2472 \times 10^{-6} \pm 0.1837 \times 10^{-6}$	-0.90315 ± 0.00122

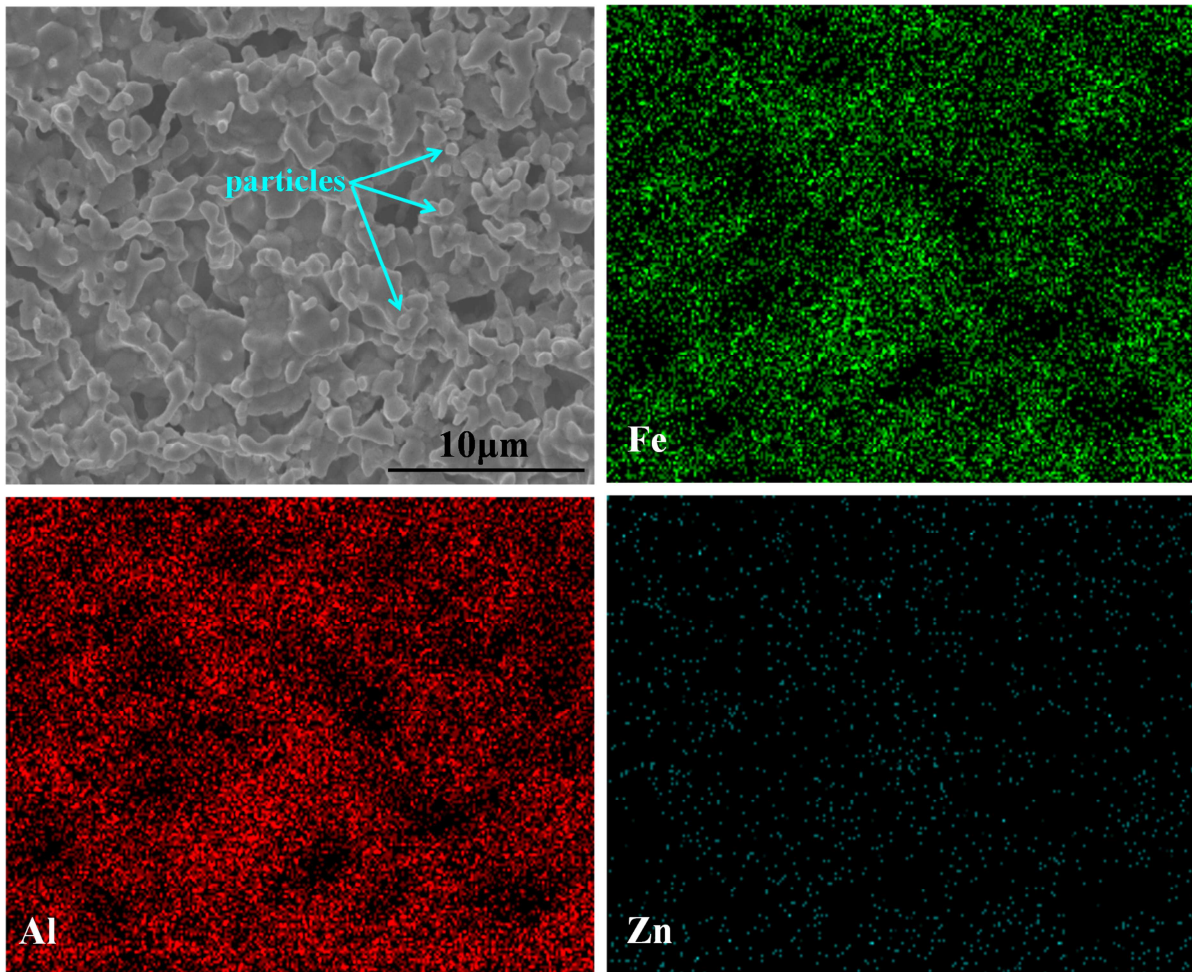




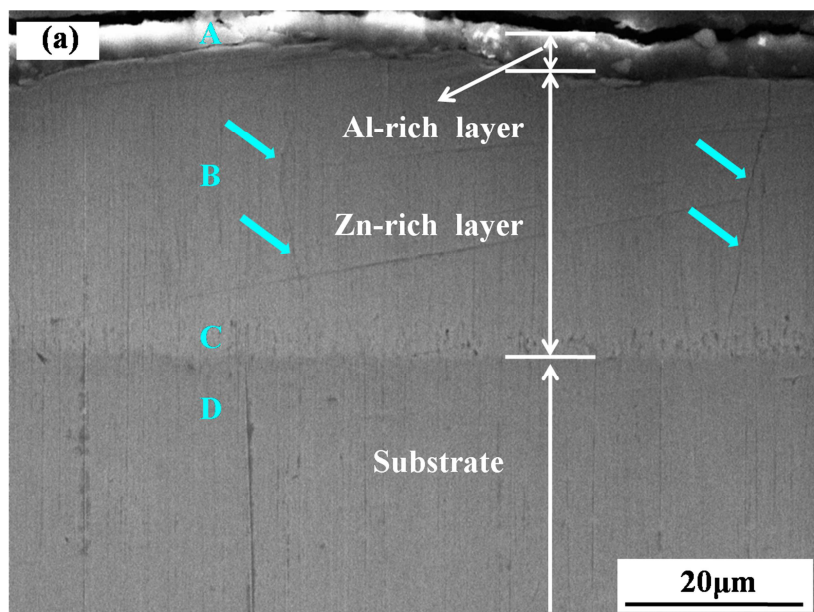


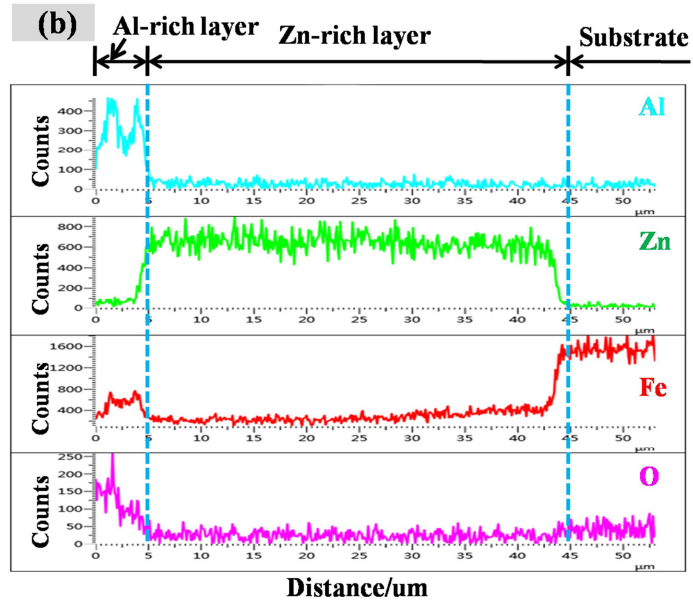


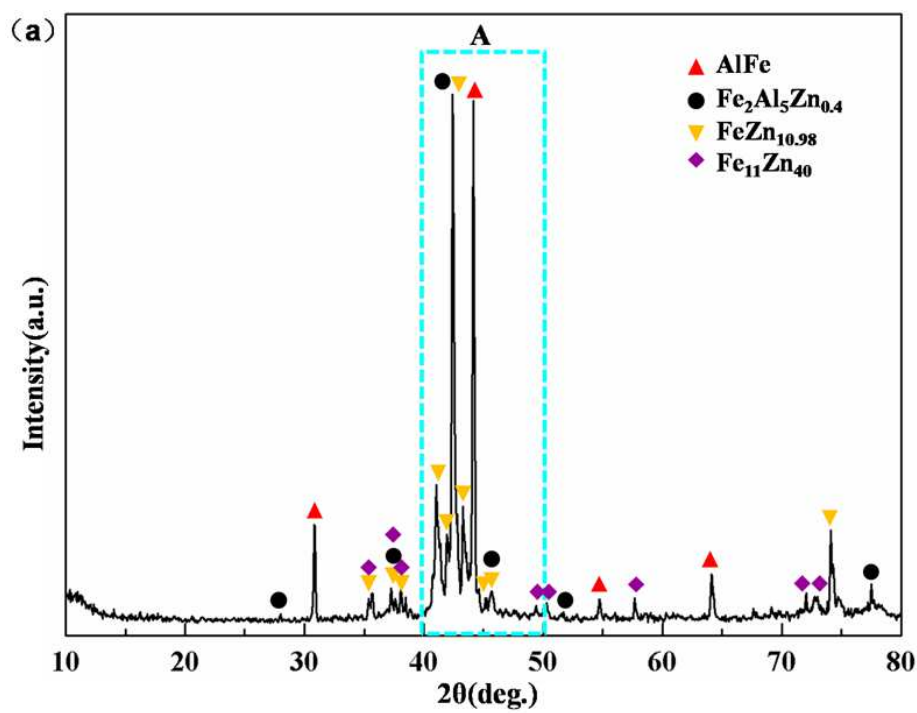


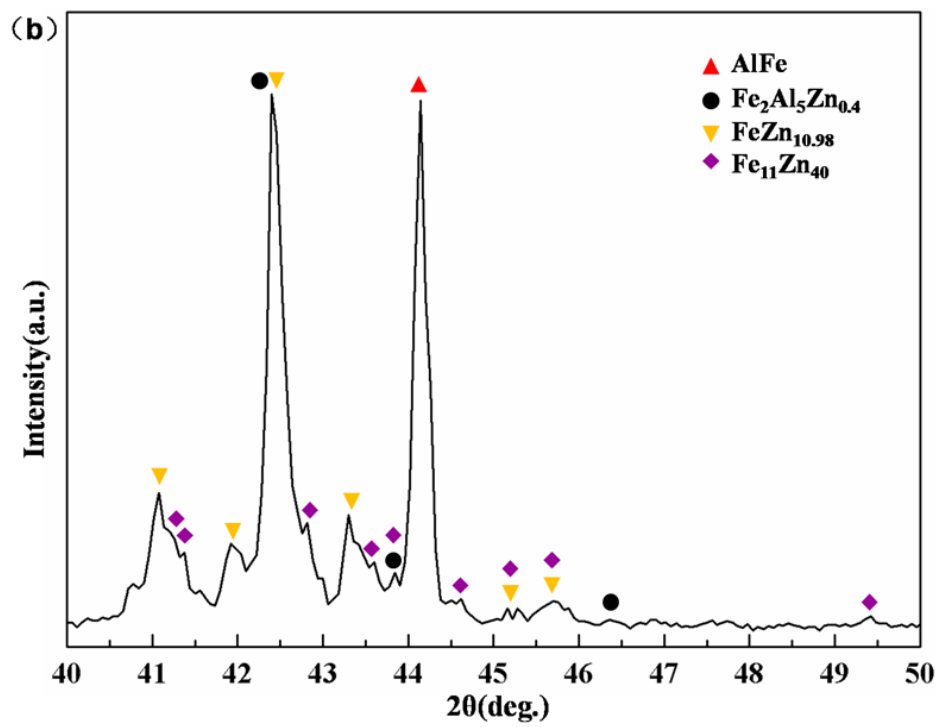


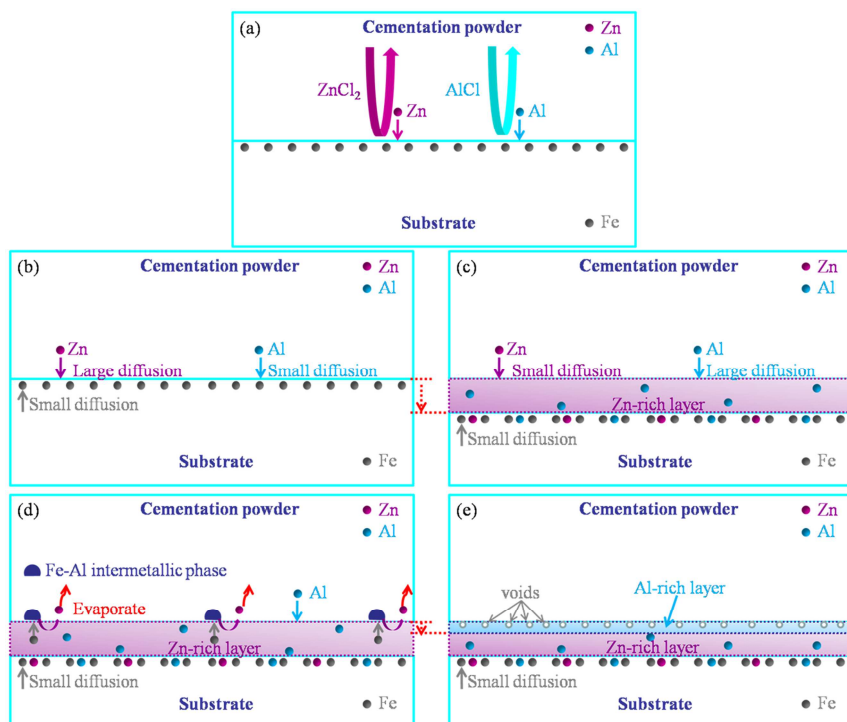
ACCEPTED

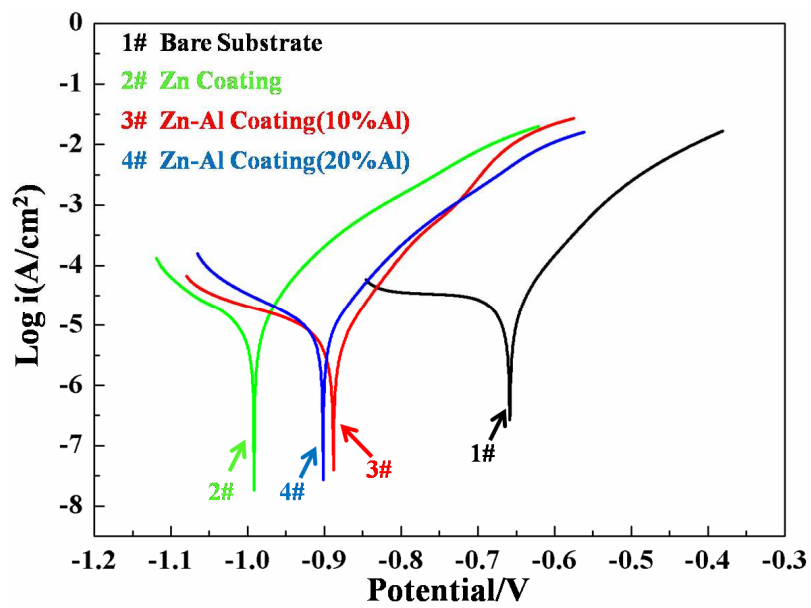


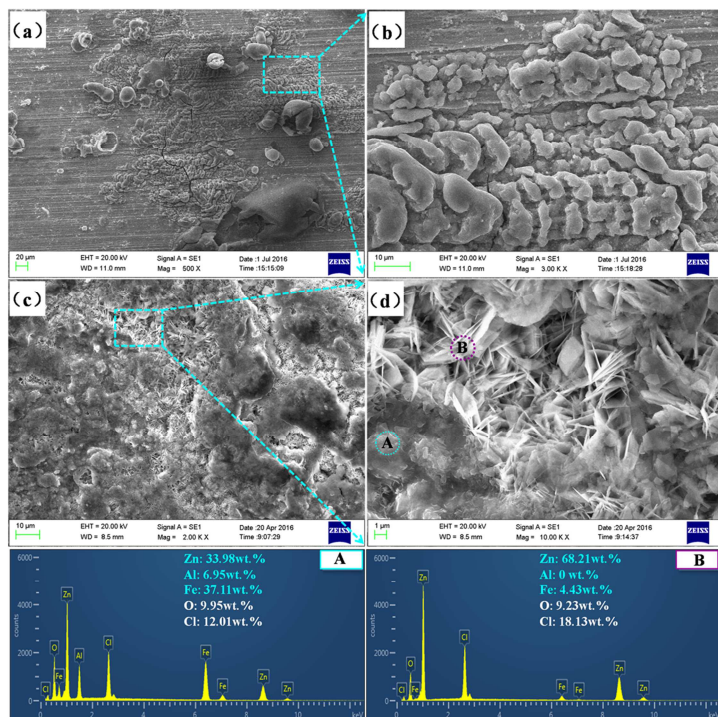












- The Zn-Al co-deposited coating was successfully produced via pack cementation.
- The effect of Al content on the microstructure of such a coating was discussed.
- The concentration evolution of Fe was analyzed.
- The evolution process and mechanism of such a coating was modeled and proposed.

ACCEPTED MANUSCRIPT